

# Development and Validation of Generic Maneuvering Flight Noise Abatement Guidance for Helicopters

James H. Stephenson  
*U.S. Army Combat Capabilities Development Command  
Aviation & Missile Center  
Hampton, VA, USA*

Eric Greenwood\*  
*Penn State University,  
University Park, PA, USA*

Michael E. Watts\*  
*Analytical Mechanics Associates, Inc.  
Hampton, VA, USA*

Kyle A. Pascioni  
*NASA Langley Research Center  
Hampton, VA, USA*

An extensive flight test campaign has been conducted to look into developing actionable advice for pilots of today's vehicles to reduce their acoustic footprints. Ten distinct vehicles were tested at three different test ranges, with nine of the vehicles' data being documented here. Twelve pairs of turning conditions were tested to determine their effect on blade-vortex interaction noise. Each turning flight condition was evaluated using the peak A-weighted, band-limited (50 Hz - 2500 Hz), sound pressure level measured throughout the maneuver. This metric was a surrogate for blade-vortex interaction noise, and the difference between the peak values of each turning pair was investigated. That peak value difference was subsequently corrected by the offset from the intended vehicle altitude at turn initiation from the actual altitude at initiation. The corrected amplitudes were investigated and grouped into six validated actionable guidance principles that can be given to pilots to immediately reduce their acoustic footprint during operations.

## Introduction

Over the past 3 years, NASA, the Federal Aviation Administration (FAA), and the US Army have conducted a series of rotorcraft acoustic flight tests that span light to medium-sized helicopters (Refs. 1, 2). One purpose of this flight test series was to determine generic maneuvering flight noise abatement guidance that can be provided to the pilots of all conventional helicopters to reduce the community noise exposure of their operations. The guidance developed focuses on controlling blade-vortex interaction (BVI) noise, as BVI noise often dominates community noise exposure metrics and is caused by a physical mechanism that the appropriately guided pilot can influence.

Helicopter noise is known to be impulsive and annoying for the local community. As a result, several localities have implemented restrictions to limit flight operations to specific times and flight paths (Refs. 3, 4). These restrictions, and potential future ones, impose an immediate requirement for noise mitigation measures that affect today's fleet of vehicles. Furthermore, learning how to develop appropriate pilot guidance today will help mitigate the acoustic footprint of future advanced air mobility vehicles.

\*Formerly NASA Langley Research Center, Hampton, VA, USA

VFS 76<sup>th</sup> Annual Forum, Virginia Beach, VA, October 6-8, 2020. This is a work of the U.S. Government and is not subject to copyright protection in the U.S. DISTRIBUTION STATEMENT A. Approved for public release.

## Background

The ability of rotorcraft pilots to reduce the acoustic impact of their operations through noise abatement procedures has been recognized since the early 1970s (Refs. 5-7). This understanding has been operationalized by Helicopter Association International's Fly Neighborly program (Ref. 8) since its establishment in 1982. Fly Neighborly aims to equip helicopter pilots with information that can be used to mitigate the acoustic impacts of their operations. During cruise, helicopter pilots are generally advised to fly at a relatively high altitude to reduce noise levels below the flight track by increasing the propagation distance. For the same reason, helicopter pilots are generally advised to climb steeply during departure in order to keep the acoustic impact confined to the area around the vertiport. Unlike cruise and departure conditions, the traditionally recommended noise abatement guidance for the approach to the vertiport varies among helicopter types.

Approach noise is frequently dominated by the onset of blade-vortex interaction. BVI occurs when the blades near the rear of the rotor disk pass close by the tip vortices formed previously near the front of the rotor disk, as shown in Figure 1. The interaction between the tip vortex and the blade causes a rapid fluctuation of the aerodynamic loads on the blades, which results in the radiation of highly impulsive, and therefore annoying, noise. Because this source of noise is strongly dependent on the relative positions of the blades and the rotor wake, it is very sensitive to changes in the operating condition of the helicopter.

The intensity and directivity of BVI noise is a function of the angle between the tip vortex and the azimuth angle of the

blade during the interaction. This interaction angle is seen in the top view geometry of the wake shown in Figure 1a, the geometry of which is primarily determined by the rotation rate of the main rotor and the true airspeed of the helicopter (Ref. 9). The intensity of BVI noise is also a strong function of the “miss distance” between the rotor disk and the shed tip vortices. When the helicopter descends along a shallow trajectory, the wake will convect below the rear portion of the rotor disk, as shown in Figure 1b, resulting in the onset of BVI noise. Increasing to a moderate descent rate, Figure 1c, the wake convects into the rotor disk, reducing the miss distance, and increasing the intensity of BVI noise. Further increases in the rate of descent, shown in Figure 1d, cause the wake to convect above the rotor disk, increasing miss distance and reducing BVI noise from the peak level seen in Figure 1c.

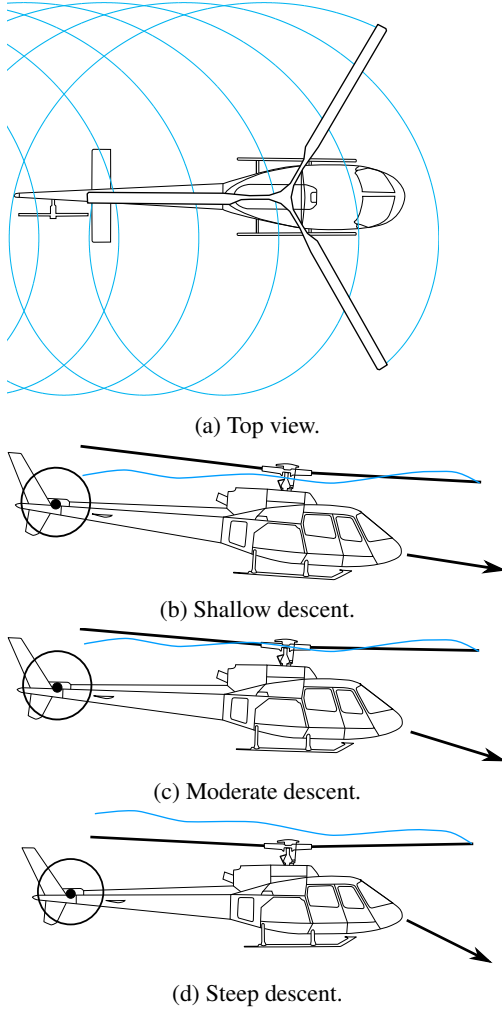


Fig. 1: The wake geometry governing BVI noise.

This miss distance is proportional to the wake skew ratio,  $\chi$ , which is the ratio of the inflow through the rotor to the flow perpendicular to the rotor tip path plane, given as:

$$\chi = \frac{\lambda_i - \mu \sin \alpha}{\mu \cos \alpha}. \quad (1)$$

Here  $\mu$  is the rotor advance ratio,  $\lambda_i$  is the induced inflow ra-

tio, and  $\alpha$  is the tip path plane angle of attack. The induced inflow ratio,  $\lambda_i$ , is strongly controlled by the rotor disk loading. Following Ref. 10, the tip path plane angle of attack can be estimated in steady flight to first order as:

$$\alpha = -\gamma - \frac{D}{W}. \quad (2)$$

Here  $\gamma$  is the flight path angle and  $D/W$  is the drag to weight ratio. Clearly, the operating conditions at which BVI occur are controlled both by the flight condition, as defined by airspeed and flight path angle, as well as characteristics specific to the type of helicopter, such as the weight, drag, and rotor geometry. As a consequence, it was thought there was no generic noise abatement guidance that could be provided for approach flight conditions.

Historically, helicopter manufacturers have worked with the Fly Neighborly program to provide operational noise data for the types that they manufacture. These data are often shown as a “fried egg” or operational noise plot, such as that shown in Figure 2a. This plot highlights the region of the helicopter’s flight envelope where intense BVI are expected to occur, so that pilots may design approach trajectories that avoid these noisy flight conditions. More recent research has identified a variety of effects that influence the noisy region of the operating envelope of helicopters of the same type, as illustrated in Figure 2b. For example, changes in air temperature and density can change the induced inflow and drag to weight ratio of a helicopter, shifting those conditions where high BVI noise levels are generated (Refs. 11–13).

Longitudinal accelerations can also influence the noisy region of the operating envelope. A positive acceleration causes the rotor to tilt forward, increasing inflow through the tip path plane. This will increase the miss distance if the rotor wake is below the rotor. Conversely, a deceleration will decrease the inflow through the rotor, increasing the miss distance if the wake is already above the rotor. Equation 2 can be modified to include the effect of longitudinal accelerations:

$$\alpha = -\gamma - \frac{D}{W} - \frac{a_x}{g}, \quad (3)$$

where  $a_x$  is the longitudinal acceleration, and  $g$  the gravitational acceleration.

Jacobs et al. (Ref. 14) exploited these effects to develop accelerating noise abatement approaches during a program sponsored by the National Rotorcraft Technology Center (NRTC), demonstrating significant reductions of the ground noise footprint over conventional approaches. Another NRTC program would later demonstrate that there is an acoustic equivalence between steady flight at one flight path angle and accelerating flight at another (Ref. 15). This allows steady flight data to be used to model accelerating approaches using Quasi-Static Acoustic Mapping (Q-SAM) to identify an effective flight path angle for accelerating flight that results in the same angle of attack during steady flight (Ref. 16). The effective flight path angle can be determined by rearranging

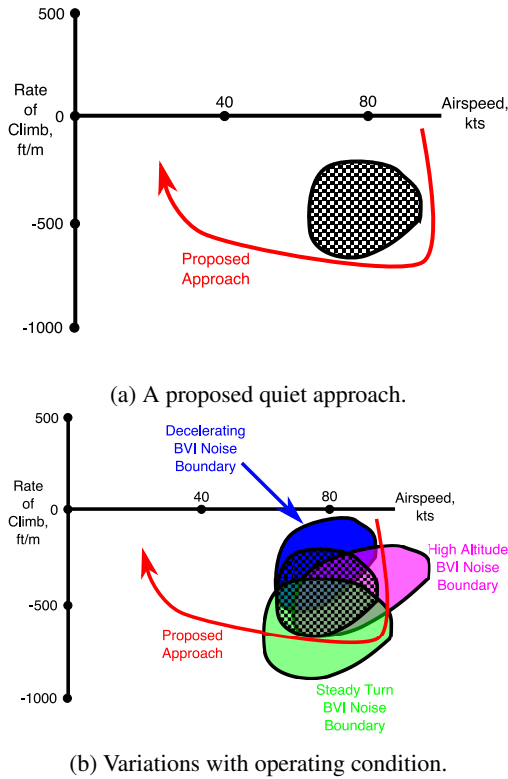


Fig. 2: “Fried egg” plots for a helicopter under (a) standard and (b) alternate operating conditions.

Equations 2 and 3, and is expressed as

$$\gamma_e = \gamma + \frac{a_x}{g}. \quad (4)$$

This method was further extended to steady turning flight at moderate bank angles by accounting for how the increase in thrust changes both the induced inflow and tip path plane angle of attack of the main rotor (Ref. 17). Flight test procedures were developed to measure the noise of steady turns using both inflight and ground-based microphone arrays. The main effect of accelerations is that BVI noise occurs at steeper flight path angles than for steady flight conditions. Follow-on flight testing under this NRTC program focused on characterizing the noise emissions during transient maneuvering flight. Strong BVI noise can be radiated to the ground during transient maneuvers for two main reasons: the first is that during transient maneuvers, the main rotor passes through a wide range of aerodynamic flight conditions, including those where the miss distance is small and intense BVI occur; the second is that the orientation of the main rotor with respect to observers on the ground changes as the attitude of the helicopter changes. This can cause intense BVI that would be directed below the helicopter in steady flight to instead propagate to observers farther from the helicopter’s ground track (Ref. 18).

The BVI noise resulting from these maneuvers could be accurately predicted by using a calibrated dynamic prescribed wake model (Ref. 19). Figure 3a compares the measured acoustic pressure time history during a fast cyclic pitch up maneuver to that predicted by the model (Fundamental Rotorcraft Acoustic Modeling from Experiments – FRAME). Of

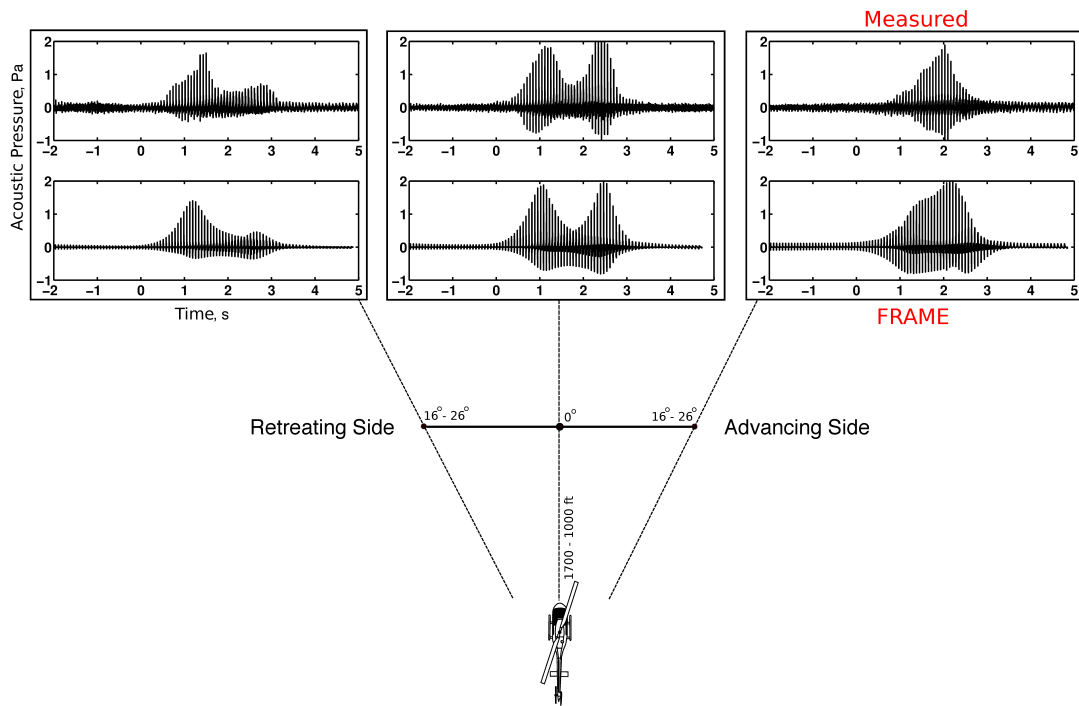
particular note is that two distinct bursts of BVI noise can be observed; the first occurs early in the maneuver ( $t = 1s$ ) and is directed toward the retreating side, the second occurs later ( $t = 2s$ ) and is directed toward the advancing side. The center observer sees both bursts. The reason that there are two bursts of BVI is explained by predicted miss distance, plotted in Figure 3b. When the helicopter begins the cyclic pitch up, the rotor angle of attack is rapidly increased, causing the vortices to convect upward through the rotor tip path plane (solid black line), and producing the first burst of BVI. This burst ends as the wake convects above the rotor. As the helicopter reduces the rate of deceleration at low speed, the angle of attack begins to decrease and the wake passes back down through the rotor resulting in the second burst. The change in airspeed, and advance ratio, changes the radiation direction of the most prominent BVI from the first burst to the second. Further study by Sickenberger (Ref. 20) indicated that the hysteresis of the wake and rotor blade dynamics was not important to capture the peak level of BVI seen during the maneuver. A quasistatic assumption can be made, with the main impact being that the peak BVI condition is predicted slightly earlier in time—on the order of a rotor revolution—than in the measured data.

A flight test conducted by DLR in 2004 characterized the noise radiation of a helicopter conducting turns and other maneuvers using a distributed array of ground based microphones (Ref. 21). These data were later used to build a database of “snapshots” of the helicopter’s noise radiation characteristics as a function of aerodynamic operating condition. This database could then be used to simulate other maneuvering flight conditions (Ref. 22). Further analysis indicated that main rotor torque correlated strongly with noise radiation and Guntzer et al. (Ref. 23) applied this approach to design low noise optimal approach conditions including maneuvering flight effects.

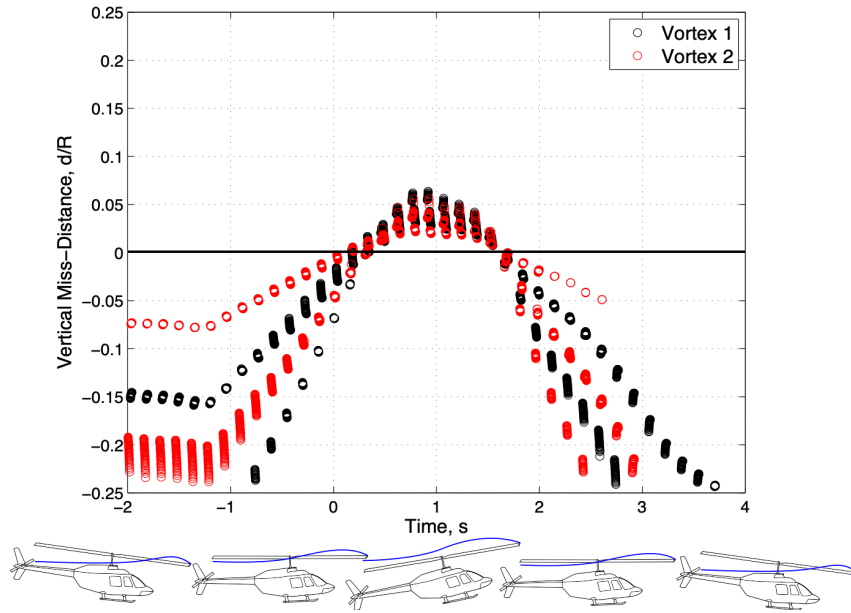
In 2011, NASA, Bell, and the US Army conducted a thorough study of the maneuvering flight acoustics of an instrumented Bell 430 helicopter (Refs. 24, 25), with a strong emphasis placed on developing a better understanding of the physics of BVI noise during maneuvering flight (Ref. 26). Review of the data showed that the characteristics of maneuvering flight BVI were substantially similar to those of steady flight BVI when normalized to the same propagation direction and distance. On this basis, the Q-SAM approach was extended to arbitrary three-dimensional maneuvers (Ref. 27), where the effective steady flight path angle for an arbitrary maneuver is:

$$\sin \gamma_e = \hat{v} \cdot \hat{n}, \quad (5)$$

where  $\hat{v}$  is the unit normal of the velocity vector in inertial coordinates and  $\hat{n}$  the unit normal of acceleration (including gravity). This equation reduces to Equation 4 for the longitudinal case after introducing the small angle assumption for the orientation of the tip path plane. Variations in rotor thrust are predicted using the FRAME model (Ref. 28). A similar quasistatic approach has since been developed using a database of noise spheres generated from first-principles predictions (Ref. 29).



(a) Measured and predicted acoustic pressure time histories.



(b) Predicted blade-vortex miss distance throughout maneuver.

Fig. 3: Measured and predicted BVI during a fast pitch up maneuver (adapted from Ref. 19). Vortex 1 and 2 are each associated with an individually modeled blade for the Bell 206B vehicle.

The extended Q-SAM approach was then applied to the AS350 helicopter to predict the acoustic impact of a wide range of possible maneuvers, with the aim of developing actionable guidance for helicopter pilots to reduce maneuver noise (Ref. 30). The candidate maneuvers were parameterized, and several hundred cases were analyzed in total. Figure 4 shows a sample of some of the results, with the A-weighted Sound Exposure Level (SEL) of level turns toward the advancing side evaluated for several different rates of acceleration along the flight path. It is evident that the decelerating turn (Figure 4a) is the loudest, producing high levels of BVI noise toward the outside of the turn. These results were distilled into the following guidance from Ref. 30:

- Decelerations, even of moderate magnitudes of 0.1 g or less, can cause significant increases in A-weighted noise levels due to the onset of BVI. Pilots should be careful to avoid the natural tendency to decelerate into other maneuvers, such as turns or pull ups, where BVI noise is more likely to occur.
- Acceleration does not lead to substantial reductions in noise during level flight, where BVI does not typically occur, but may still be useful to increase the “miss distance” margin from BVI-prone flight conditions during maneuvers, such as the roll-in to a turn. However, acceleration should not be sustained throughout the duration of turns or other maneuvers as the increased flight speed will result in higher noise radiated ahead of the helicopter.
- Noise levels on the outside of a turn are generally higher than toward the inside of a turn, due to the banking of the helicopter directing main rotor loading and tail rotor thickness noise toward the outside of the turn. Noise levels during turning flight are higher than for similar straight line flight conditions. Turns should be avoided near noise sensitive areas; when turns must be made near noise sensitive areas, the acoustic impact is minimized by keeping the noise sensitive region toward the inside of the turn.
- BVI noise caused by the roll-in or out of a turn is increased for turns toward the advancing side of the rotor. Advancing side turns should not be combined with deceleration or descents when possible. However, advancing side turns are not much louder than retreating side turns during accelerating or climbing turns, where BVI is more easily avoided.
- Rotor harmonic noise levels are relatively insensitive to the rate of climb, although the initial rate of increase of the flight path angle should be limited to avoid unnecessary deceleration. Steeper climbs allow the helicopter to

increase altitude more quickly, reducing noise levels directly beneath the flight track. However, attenuation of noise levels has diminishing returns with increasing altitude due to the nature of spherical spreading losses. Moreover, increased altitude provides little noise benefit to observers who are far from the flight path.

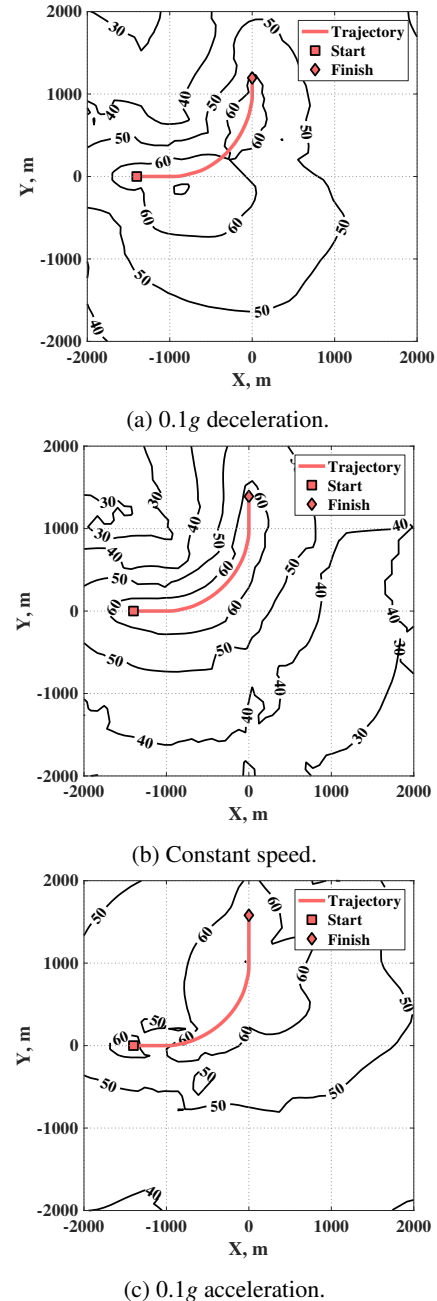


Fig. 4: Sound Exposure Level contours (dBA) for turns toward the advancing side from 80 knots indicated airspeed (adapted from Ref. 30).

Although this guidance was developed from analysis of a very wide range of flight conditions, the underlying data were

for a single type of light helicopter, and the effectiveness of the procedures had not been experimentally validated for a wider range of types. Although approach procedures must be tailored to the specific type of helicopter—if not configuration and operating environment of the vehicle at the time of use—transient maneuvers often start from a level flight condition where the rotor wake normally convects well below the rotor. This means that there is the potential to develop more generic guidance for transient maneuvers focused on keeping the rotor well below the wake throughout the maneuver, thus increasing miss distance and reducing the occurrence of objectionable BVI. Validating and extending this guidance across a range of helicopters formed the basis of the maneuvering flight test plan for the joint NASA/FAA/Army tests conducted for light helicopters in 2017 (Ref. 1) and extended to medium helicopters in 2019 (Ref. 2).

## Flight Test Descriptions

Two flight test programs were undertaken to determine flight procedures for today's fleet of vehicles. The first flight test program was reported by Watts et al. (Ref. 1) and included testing six light helicopters at two locations. The helicopters included in the test were the Robinson R44, Robinson R66, Bell 206L3, Bell 407, Airbus AS350B, and Airbus EC130. These helicopters were selected due to their prevalence in noise sensitive areas across the United States and because they represent technology pairs, allowing the acoustic differences between older and newer generations of helicopters to be assessed. The R44 and R66 pair differed primarily in type of engine (piston versus turbine), the Bell 206 and Bell 407 pair investigated differences associated with main rotor hub design (teetering versus soft-in-plane hingeless) and blade count (two versus four), and the AS350 and EC130 primarily investigated the effects of antitorque system (tail rotor versus Fenestron). These vehicles were tested either at Eglin Air Force Base, FL or Amedee Army Airfield, CA, based on local availability of the vehicles. In all cases, both helicopters of a pair were tested at the same location.

The second flight test program is being reported in Pascioni et al. (Ref. 31), focusing on medium-sized helicopters. This flight test was conducted at Coyle Field, NJ and included a Bell 205 "Huey," AgustaWestland AW139, Sikorsky S-76D, and a Eurocopter MH-65. Each test included on-board vehicle tracking and inertial navigation data synchronized with a large ground-based microphone array. Details of the on-board vehicle instrumentation and data collection can be found in Refs. 1 and 2.

## Flight Maneuver Descriptions

The same specific set of acoustic data were acquired for each aircraft. Hover, steady descent, level, and ascent flights were flown at various flight conditions in order to develop and validate noise abatement approaches specific to that type and to acquire source noise data that can be used in modern acoustic planning tools, such as the Advanced Acoustic Model. The

test procedures for these conditions are described more fully in Refs. 1 and 2. The focus of this paper identifies and validates low noise maneuvering flight procedures that are applicable to all conventional helicopters. The flight conditions developed and flown to meet this objective are as follows:

- *Constant speed steady level turns.* These conditions represent the baseline turning flight maneuvers. The pilots were instructed to approach the acoustic array in an established level flight condition at a specified airspeed. At the designated point, they were told to roll normally to the indicated bank angle and hold that angle until at least 90° of heading change. Then they could roll out of the turn and prepare for the next condition.
- *Constant torque steady level turns.* These conditions were designed to represent ways in which pilots might "naturally" depart from a nominal maneuver when not closely flying by instruments. The conditions were flown with the same instructions as the baseline maneuvers, except that the pilots were instructed to maintain constant collective pitch (or rotor torque). Variations of these maneuvers were flown where pilots were instructed to maintain altitude and allow airspeed to decrease or to maintain airspeed and allow altitude to decrease.
- *Turns with acceleration during the roll-in.* These conditions were intended to control the BVI miss distance during the initial transient roll-in to the turn by establishing an accelerating (or decelerating) flight condition during turn entry. The pilots were instructed to establish a constant acceleration rate at a designated point prior to the array. At the designated maneuver point, the pilot would roll-in to the turn (as in the baseline condition) but maintain the specified acceleration until the target bank angle for the maneuver was achieved.
- *Turns from climbing and descending flight.* These conditions were intended to simulate maneuvers that might be conducted on approach or departure. Descending or climbing flight is expected to influence the miss distance during the roll-in in a similar manner to decelerating or accelerating flight. During these conditions, the pilot would establish a constant speed, constant climb (or sink) rate condition at the designated point, and then enter the turn at the designated maneuver point. After establishing the target bank angle, the descent could be arrested.
- *Turns from descending flight with accelerations or decelerations through the roll-in.* These conditions were designed to provide alternative strategies for conducting turns during approach conditions, by using acceleration to control miss distance. The condition is established in the same manner as the descending turn, except that an acceleration or deceleration is established along the flight path angle at the designated point.

Acceleration, climb, descent, and turn indications were provided to the pilots by adjusting the angle of lamps on a

Precision Approach Path Indicator (PAPI) system, such that the lights would appear to turn from red to white when the pilot flew by the designated point at the target altitude. The lamp angles were adjusted for each flight condition, so that the expected turn radius would bring the aircraft over the desired portion of the acoustic array. However, in some cases, error in the flight altitude or lamp malfunctions caused the pilots to miss the desired flight conditions. In these cases, the pilots would revert to manual guidance where fixed markers on the ground were used to designate a common set of condition set up and turn indications for all maneuvers.

### Microphone Array Descriptions

Each of the three test locations possessed unique physical limitations, which prevented the deployment of a common microphone array pattern. At each test location, the microphone arrays were designed to capture as much of the ground footprint as possible, in order to maximally evaluate the community noise exposure. The test location at Coyle field was significantly smaller than either of the 2017 test sites. Based on experience from the 2017 tests, the array was arranged to cover the maximum possible sideline distance across the flight track, instead of providing more coverage along the flight path direction.

The microphone array for each of the three locations can be seen in Figure 5. It can be seen that the arrays span up to 6700 feet in the flight path direction ('X') and 4000 feet normal to the flight path ('Y'). Descriptions of the data acquisition systems are located in Refs. 1 and 2.

At each location, a GRAS 67AX  $\frac{1}{2}$ " embedded ground board microphone was radio controlled and sampled at 25 kHz. During some flights past our microphone array, the microphone data recording was corrupted either due to radio transmission issues or other internal malfunctions. On the acoustic contour maps provided in subsequent figures, each microphone location is marked by an open circle. When an error which prevented accurate data collection occurs, the marker position for that microphone will not be shown on the affected contour map.

### Guidance Development

A detailed analysis was conducted of the ground-based microphone array data to determine the effects of turning flight on perceived noise levels at the ground. Combinations of various turn conditions were investigated to determine if one condition resulted in a quieter acoustic footprint than another. The acoustic metric used in this analysis was the maximum of the A-weighted, band-limited (50 Hz - 2500 Hz), sound pressure level as measured on the ground at any point during the maneuver ( $L_{A,max}$ ).

A detailed investigation of the vehicle flight track was also conducted in order to ensure that the pilot accurately flew the trajectory prescribed for each data run. Each flight path maneuver was executed multiple times during testing, while only

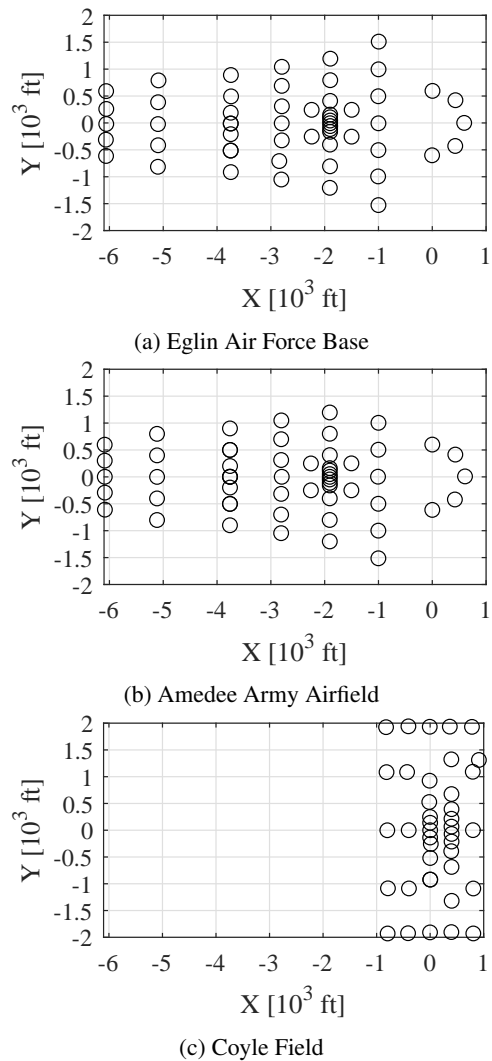


Fig. 5: Microphone layout for (a) Eglin Air Force Base, (b) Amedee Army Airfield, and (c) Coyle Field. Circles are used to represent each microphone's location.

the data from the flight path that best met the desired condition are used here. Determination for the "best" flight path was conducted through a visual inspection of the flight track and inertial vehicle data, to ensure the pilot executed the desired maneuver, at the desired rate, and at the proper location for the microphone array to capture the data. Unfortunately, MH-65 data did not meet the requirements for use in this document and minimal AW139 data are available. Due to the aforementioned issues with providing maneuver guidance, many conditions were executed too soon for the truncated Coyle Field array (Figure 5c) to adequately capture the acoustic footprints and make an accurate evaluation. Documentation of all of the flown maneuvers can be found in Watts et al. (Ref. 1), which documents the Eglin AFB and Amedee Army Airfield flight tests, and Pascioni et al. (Ref. 2), which documents the Coyle Field flight test.

## Data Analysis

A subset of the acoustic results from some maneuver combinations of individual vehicles are presented here, while a complete list can be found in the previously mentioned technical memoranda. Figure 6 presents the  $L_{A,max}$  contour plot of a Bell 206 during a steady, level, left-hand 35° turn. Also presented in Figure 6 is the ground speed, altitude above microphone reference height, and roll angle as a function of vehicle position. The contour levels presented in the figure range from 60 to 80 dBA, and it can be seen that the speed of the vehicle was held fairly constant around 90 knots, altitude was held constant at approximately 550 feet, and the maneuver was held until a 35° roll was achieved. The  $L_{A,max}$  contour plot shows a peak amplitude of 73.4 dBA at an (X,Y) location of (-1905, 800) feet for this maneuver.

When interpreting the contour plots within this document, it should be noted that only the values at the open circles, which denote the locations of active microphones, are accurate. The contour levels between each microphone location are interpolated results to ease visualization, and those values will change depending on interpolation scheme. The peak amplitudes identified in this study are from the measured values, and not the interpolated contours, so are not subject to the interpolation scheme.

A comparable maneuver to Figure 6 can be seen in Figure 7. In this figure, the pilot executes a descending, left-hand 35° turn. The pilot descends at approximately -6° flight path angle, from an altitude of 500 feet to approximately 380 feet. During the execution of this run, the pilot incidentally slows the vehicle from 90 knots to 75 knots. However, the acoustic impacts of this maneuver are very evident in the  $L_{A,max}$  contour plot, where a significant portion of the microphone array recorded values above 75 dBA, with a maximum value of 81.6 dBA measured at an (X,Y) location of (-2800, 0) feet. Compared to Figure 6, this maneuver resulted in a measured peak amplitude increase of 8.2 dBA. From this, it can be concluded that a descending left-hand turn in the Bell 206 vehicle is louder than a steady, level, left-hand turn. This increase in noise is caused by a reduced BVI miss distance, a result of the descending flight.

An investigation of the Bell 407 vehicle for the same combination of left-hand turns as just investigated, results in a maximum  $L_{A,max}$  increase of 7.5 dBA. Perhaps more interestingly, this vehicle can be investigated for similarly paired maneuvers with a right-hand turn. Figures 8 and 9 show a steady, level, right-hand turn, and a descending right-hand turn, respectively. It can be seen in Figure 8 that the level right-hand turn was executed at approximately 82 knots and an altitude of close to 600 feet. The resulting dBA contour plot shows a maximum recorded  $L_{A,max}$  of 71.9 dBA.

In Figure 9, it can be seen that the pilot descends from 600 feet to approximately 380 feet, and maintains a speed of close to 75 knots. Again, for this condition, it can be seen that a significant portion of the microphone array recorded values above 75 dBA, with a maximum value of 79.4 dBA measured

at an (X,Y) location of (-2800, 0) feet. Compared to Figure 8, this maneuver resulted in a measured peak amplitude increase of 7.5 dBA, which was similar to the results from the left-hand turn. Again, it can be concluded that a descending right-hand turn in the Bell 407 vehicle is louder than a steady, level, right-hand turn; and that the noise increase is a direct result of the reduced BVI miss distance during descending flight.

Similar data can be investigated from the Coyle Field flight test where medium-weight vehicles were investigated. Figure 10 shows the results from an accelerating, level, right-hand 35° turn of the S-76D vehicle. The contour levels presented in the figure range from 65 to 85 dBA, and the effect of the truncated microphone array is clearly evident. It can be seen that the speed of the vehicle accelerated from 90 knots to approximately 102 knots with an acceleration of approximately 0.05g, altitude was held constant at approximately 400 feet, and the maneuver was held until a 35° roll was achieved. The  $L_{A,max}$  contour plot shows a peak amplitude of 79.1 dBA at an (X,Y) location of (0, -140) feet for this maneuver.

A comparable maneuver can be seen in Figure 11. In this figure, the pilot executes a decelerating, right-hand 35° turn. It can be seen that the speed of the vehicle decelerated from 75 knots to approximately 70 knots, altitude was held constant at approximately 400 feet, and the maneuver was held until a 35° roll was achieved. However, the acoustic impacts of this maneuver are less clearly evident in the  $L_{A,max}$  contour plot, where a peak amplitude of 80 dBA at an (X,Y) location of (-400, 0) feet for this maneuver was measured. Compared to Figure 10, this maneuver resulted in a measured peak amplitude increase of 0.9 dBA. From this, it cannot be concluded that a decelerating right-hand turn in the S-76D is louder or quieter than an accelerating right-hand turn. Here, the wake is well below the rotor at the initiation of the maneuver, probably because of a high disk loading and low drag to weight ratio, so the BVI miss distance remains large and the effect of deceleration is less noticeable.

An investigation of the Bell 205 vehicle for the same combination of right-hand turns as just investigated, results in a maximum  $L_{A,max}$  increase of 13.3 dBA. Continuing the investigation of maneuver noise, Figures 12 and 13 show an accelerating, level, left-hand turn, and a decelerating, level, left-hand turn, respectively. It can be seen in Figure 12, the accelerating left-hand turn was executed with a speed change from 90 knots to 95 knots, at an altitude of close to 400 feet. The resulting dBA contour plot shows a maximum recorded  $L_{A,max}$  of 80.3 dBA.

Figure 13 shows the results from the decelerating, level, left-hand 35° turn of the Bell 205 vehicle. The pilot decelerates from a speed of 82 knots to 65 knots, at an altitude of close to 350 feet. The resulting dBA contour plot shows a maximum recorded  $L_{A,max}$  of 85.3 dBA at an (X,Y) location of (0, -140) feet, which produces a measured peak amplitude increase compared to Figure 12 of 5 dBA. It can be concluded that the longitudinal acceleration for this maneuver has significantly affected the effective flight path angle, reducing the BVI miss distance, and increasing the acoustic emissions.

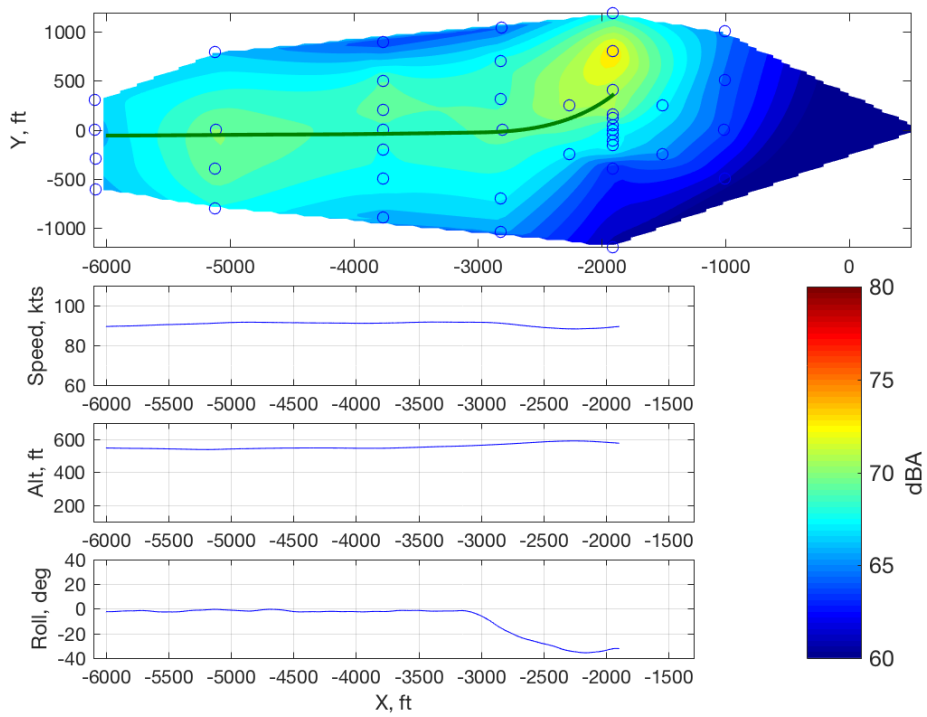


Fig. 6: Bell 206 vehicle executing a steady, level, left-hand 35° turn.

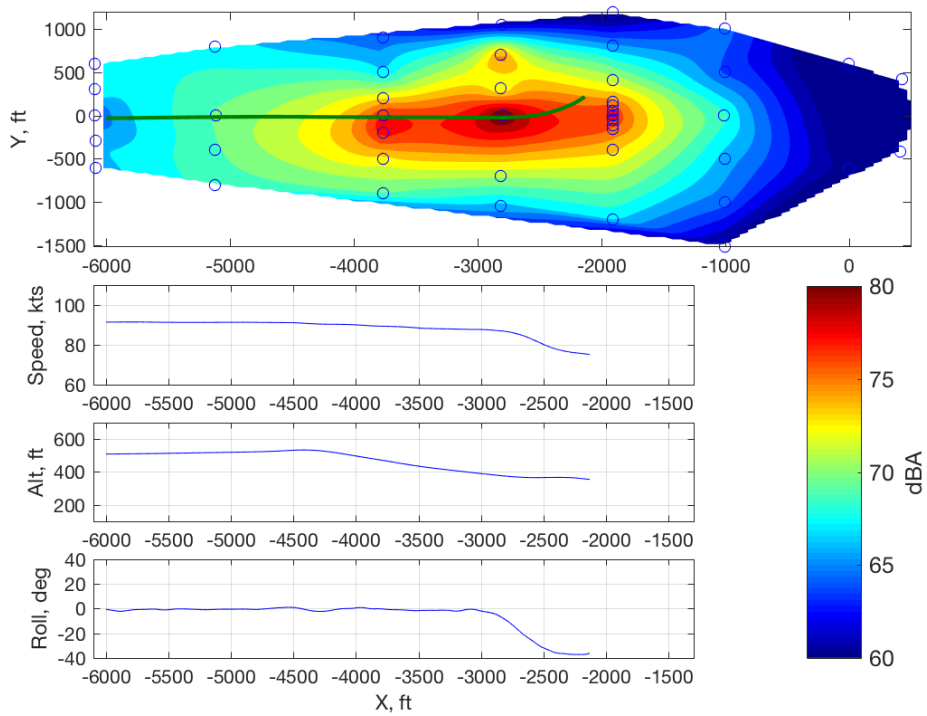


Fig. 7: Bell 206 vehicle executing a descending, left-hand 35° turn.

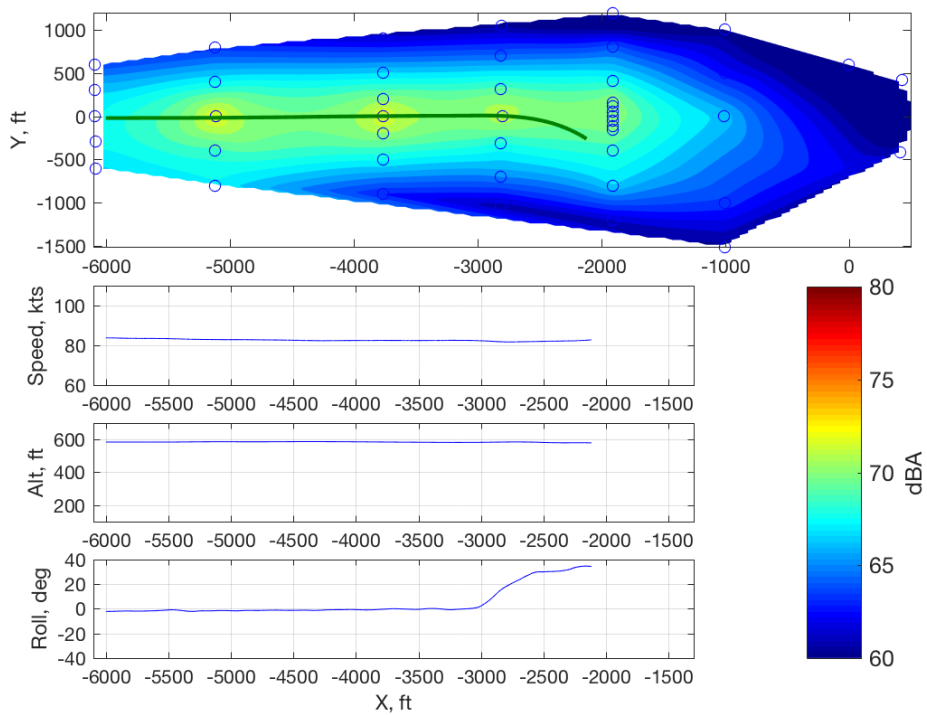


Fig. 8: Bell 407 vehicle executing a steady, level, right-hand 35° turn.

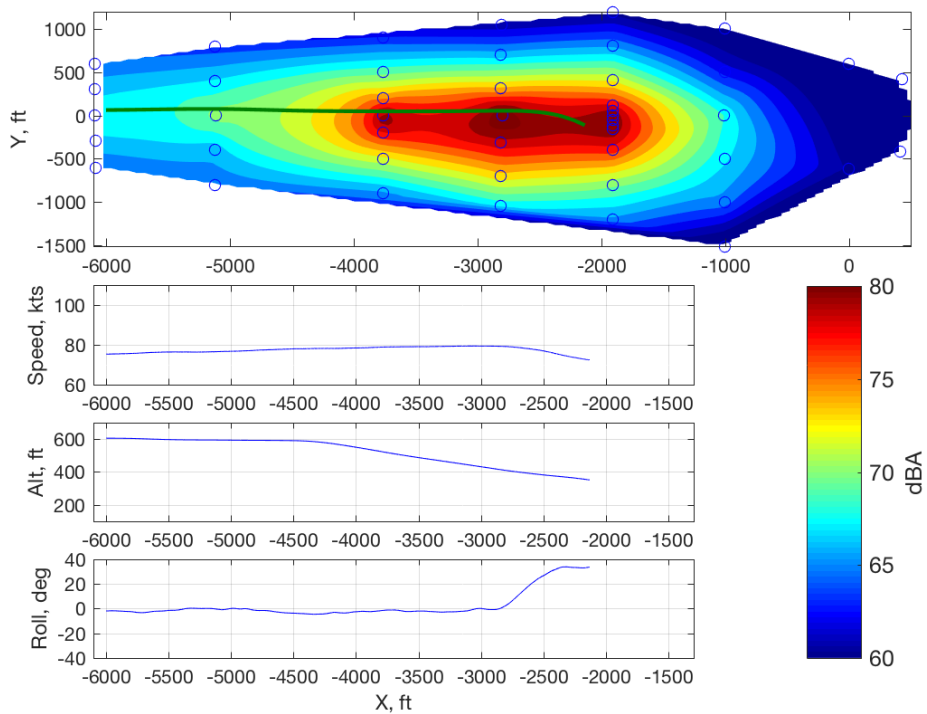


Fig. 9: Bell 407 vehicle executing a descending, right-hand 35° turn.

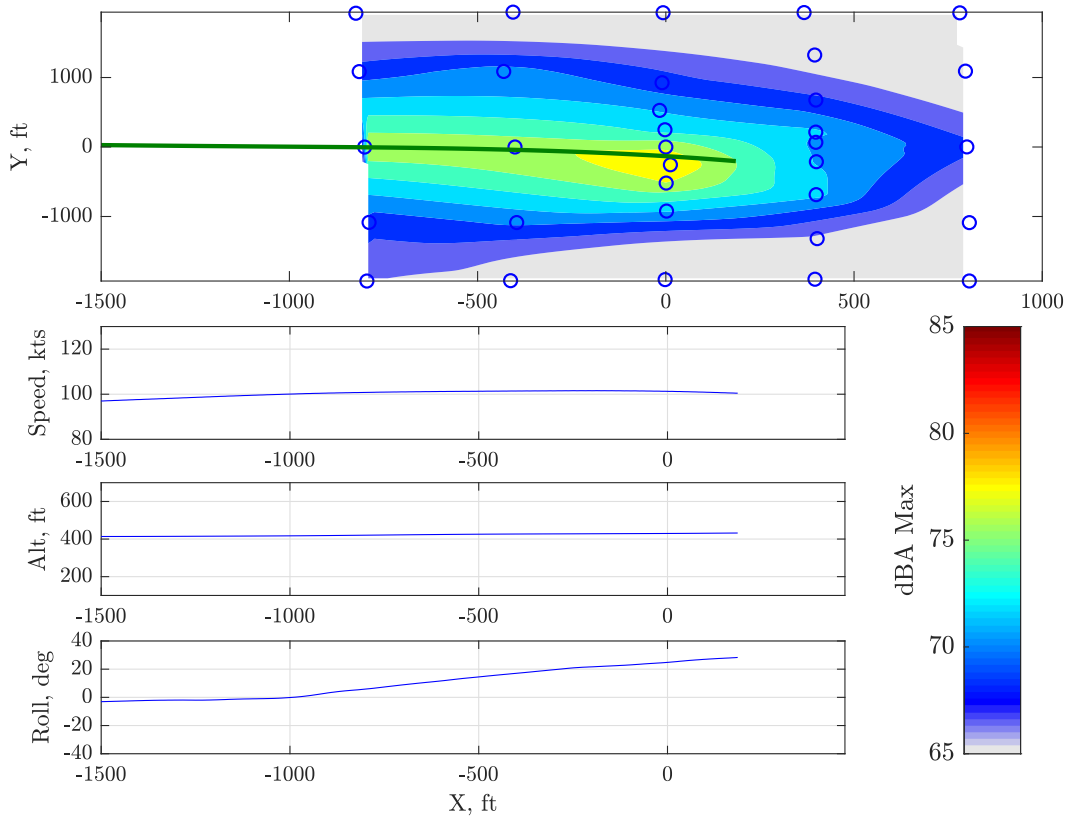


Fig. 10: S-76D vehicle executing an accelerating, level, right-hand 35° turn.

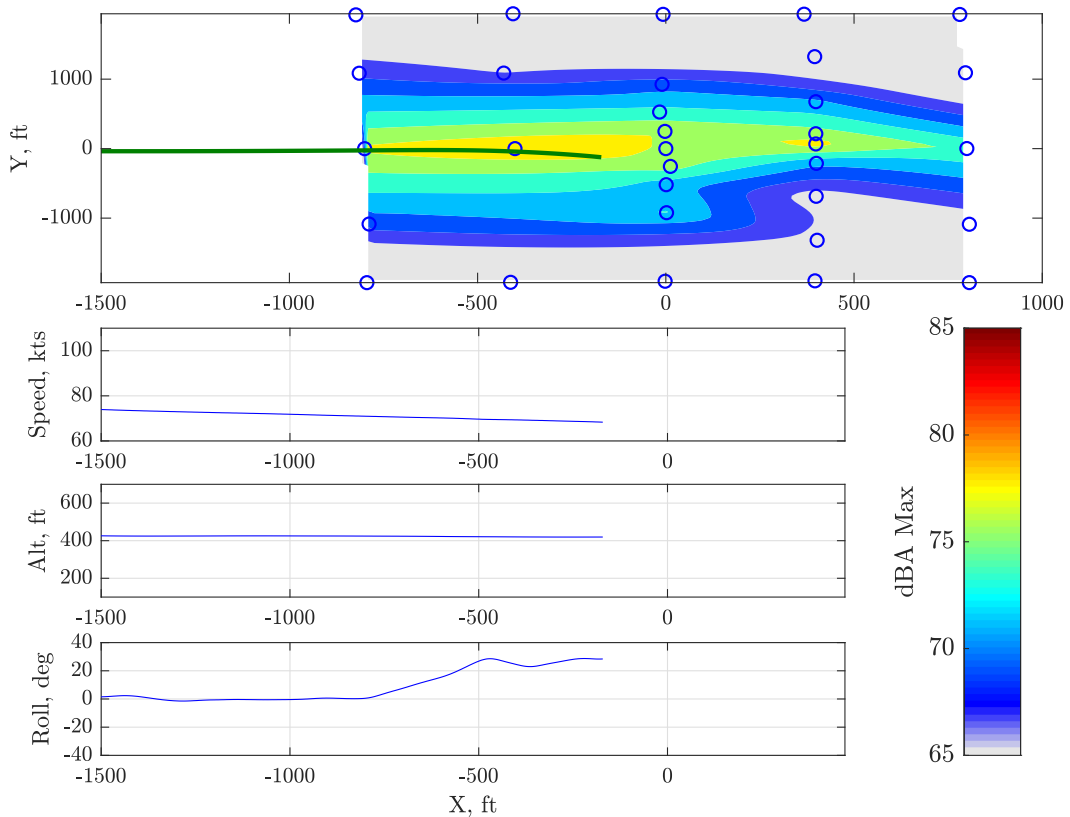


Fig. 11: S-76D vehicle executing an decelerating, level, right-hand 35° turn.

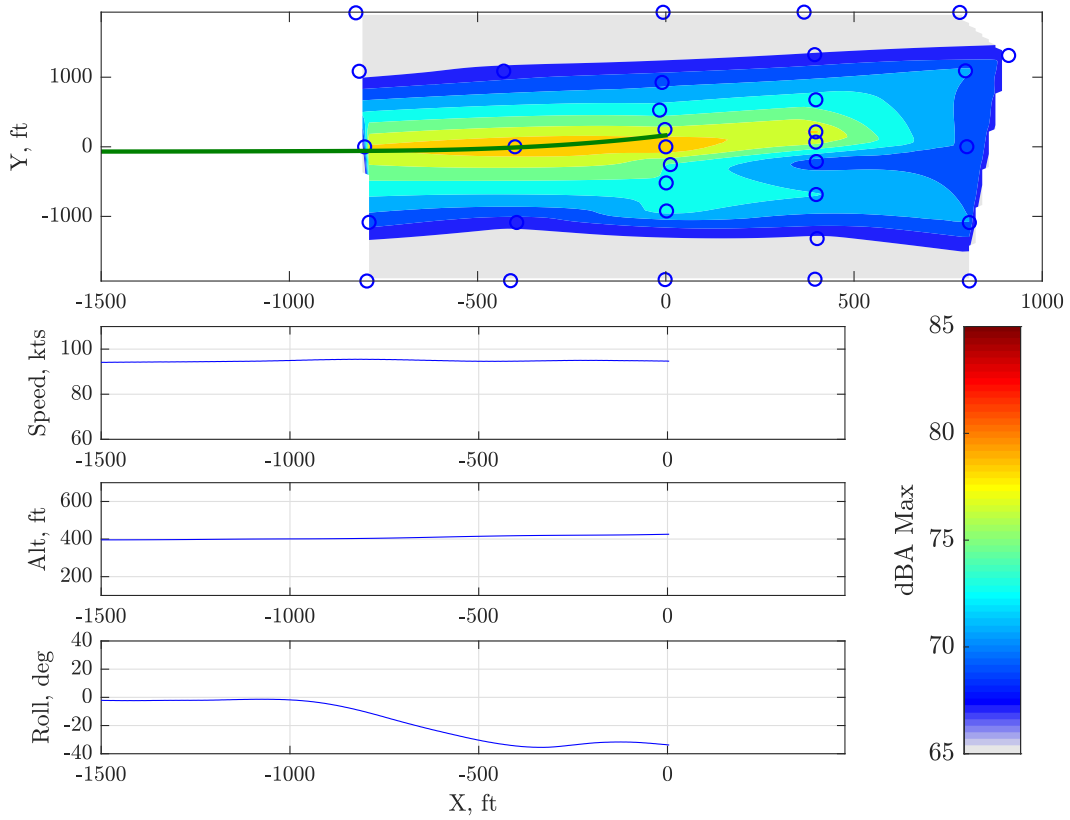


Fig. 12: Bell 205 vehicle executing an accelerating, level, left-hand 35° turn.

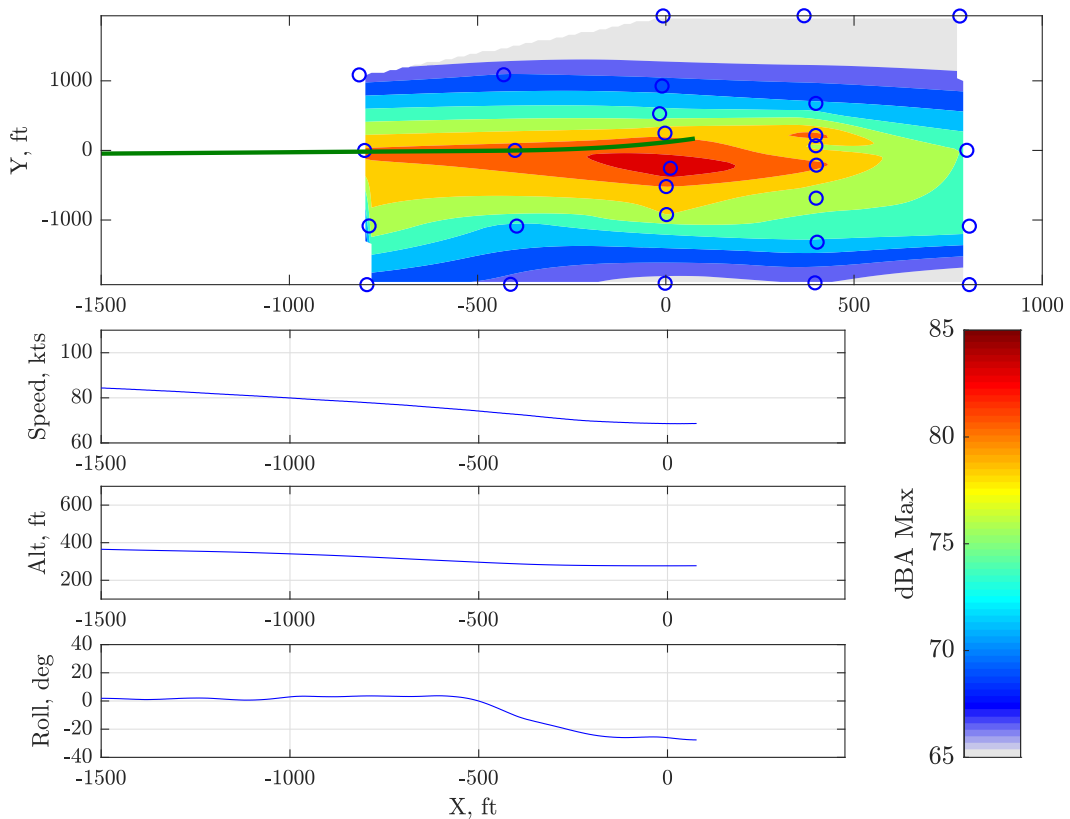


Fig. 13: Bell 205 vehicle executing a decelerating, level, left-hand 35° turn.

Table 1: Validity of the maneuver general rules of thumb for six lightweight helicopters and three medium-weight helicopters executing turning maneuvers. The colors denote if the statement is **True**, **False**, or **Neutral**; white boxes denote conditions where no data are available. Values in each cell are the measured difference in peak  $L_{A,max}$  value between condition pairs. All turns were held until a  $35^\circ$  roll was executed, unless otherwise noted.

	Condition	R44	R66	Bell 206	Bell 407	AS350	EC130	Bell 205 (25° roll)	Bell 205	S-76D	AW139
A	Retreating Side Turns are Quieter than Advancing Side Turns at Constant Speed	-0.3	0.8	-0.8	0.3	-0.1		-1.3	-0.4	-0.2	-0.6
B	Retreating Side Turns are Quieter than Advancing Side Turns at Constant Torque		-3.2		0.0	-2.0	0.9		0.1		-1.2
C	Left Turns in Level Flight are Quieter when Accelerating than Decelerating	-4.3	-1.3	-1.8	-6.1	-12.4	-0.4	-5.3	-5.0	-2.7	
D	Right Turns in Level Flight are Quieter when Accelerating than Decelerating	-11.9	-9.2	-4.8	-1.9	-2.9	0.9	-7.4	-13.3	-0.9	
E	Left Turns in $-6^\circ$ Descending Flight are Quieter when Accelerating than at Constant Speed	5.7		-0.3	2.2	-0.4		1.0	1.5	0.1	
F	Right Turns in $-6^\circ$ Descending Flight are Quieter when Accelerating than at Constant Speed	10.7	-4.3	2.0	2.5	4.0	1.5	2.6	-0.7		
G	Left Turns are Quieter in Level Flight than in $-6^\circ$ Descending Flight	-0.9	-1.8	-8.2	-7.5	-13.2		0.5	-1.1	-6.6	
H	Right Turns are Quieter in Level Flight than in $-6^\circ$ Descending Flight	-3.0	-14.1	-7.0	-7.4	-6.4	-12.8	1.2	-9.3	-7.0	
I	In $-6^\circ$ Descending and Accelerating Flight, Retreating Side Turns are Quieter than Advancing Side Turns	-2.5	-11.5	0.4	0.3	-6.8	-1.1	-0.6	-8.6	-0.5	
J	In $-3^\circ$ Descending Flight, Retreating Side Turns are Quieter than Advancing Side Turns	-7.6		-1.9	0.0	-2.3		-2.2	-6.4		
K	In $-6^\circ$ Descending Flight, Retreating Side Turns are Quieter than Advancing Side Turns	-2.6	-3.1	-0.3	-1.8	0.4	-4.1	-4.5	-0.2	-1.3	
L	In $-9^\circ$ Descending Flight, Retreating Side Turns are Quieter than Advancing Side Turns	-0.9	-0.1	-1.4	-4.8	-3.6	-4.4				

### Table Development

Several tables have been developed in an effort to compress the significant amount of information available from all of the vehicles measured for many of the maneuver combinations. Furthermore, the maneuver combinations have been grouped as shown in the previous section, in order to attempt to develop general rules of thumb as guidance that can be given to helicopter pilots in order to fly more neighborly.

Table 1 contains a breakdown of the 12 turning flight condition pairs that were examined, and a determination of whether the condition resulted in an improved acoustic footprint or not. If the difference between peak  $L_{A,max}$  between conditions in the second column of Table 1 was more than 1 dB quieter, the statement was deemed ‘true’ and is colored green. If the difference between conditions resulted in a  $L_{A,max}$  value more than 1 dB louder, the statement was deemed ‘false’ and is colored red. If neither condition was met, then the statement was ‘neutral’ and is colored blue. Also included

in each cell is the measured peak  $L_{A,max}$  dBA difference value between the condition pairs. Due to time, vehicle, and location constraints, data for some conditions were not measured, and so no comment can be made as to the validity of the condition for those cases, such as condition (B) for the R44 vehicle or conditions (C) through (L) for the AW139.

The condition pair figures provided in the previous section were selected in order to help interpret the results provided in Table 1. Figure 6 shows an 8.2 dB reduction in  $L_{A,max}$  when conducting a steady, level, left-hand turn in a Bell 206 versus descending during the turn as seen in Figure 7. This led to condition (G) in Table 1 for the Bell 206 vehicle being marked ‘true’ and a value of -8.2 is provided in that cell. Similarly, Figures 12 and 13 lead to condition (C) for the  $35^\circ$  roll of the Bell 205 vehicle being marked green with a -5.0 dBA value recorded.

One of the major issues with flight testing is executing the perfect maneuver, by appropriately varying the speed, altitude, heading of the vehicle and initiating the maneuver at the

Table 2: Validity of the maneuver general rules of thumb for six lightweight helicopters and three medium-weight helicopters executing turning maneuvers. The colors denote if the statement is **True**, **False**, or **Neutral**; white boxes denote conditions where no data are available. Values in each cell are the measured difference in peak  $L_{A,max}$  value between condition pairs and have been corrected for variation in altitude height at turn initiation. All turns were held until a  $35^\circ$  roll was executed, unless otherwise noted.

	Condition	R44	R66	Bell 206	Bell 407	AS350	EC130	Bell 205 ( $25^\circ$ roll)	Bell 205	S-76D	AW139
A	Retreating Side Turns are Quieter than Advancing Side Turns at Constant Speed	-0.4	0.6	-0.9	0.1	0.2		-0.9	-0.5	-0.1	-0.7
B	Retreating Side Turns are Quieter than Advancing Side Turns at Constant Torque		-3.7		-0.2	-2.1	0.8		0.6		-1.1
C	Left Turns in Level Flight are Quieter when Accelerating than Decelerating	-4.3	-0.8	-3.0	-5.5	-12.7	-0.3	-5.6	-2.6	-3.2	
D	Right Turns in Level Flight are Quieter when Accelerating than Decelerating	-12.0	-9.3	-5.8	-2.9	-2.9	0.8	-7.3	-11.2	-1.0	
E	Left Turns in $-6^\circ$ Descending Flight are Quieter when Accelerating than at Constant Speed	4		-1.2	1.6	-0.3		1.6	3.1	0.2	
F	Right Turns in $-6^\circ$ Descending Flight are Quieter when Accelerating than at Constant Speed	9.0	-4.6	1.6	1.8	4.0	3.1	2.3	-0.7		
G	Left Turns are Quieter in Level Flight than in $-6^\circ$ Descending Flight	-1.2	-1.5	-5.7	-5.1	-11.3		0.9	0.5	-0.9	
H	Right Turns are Quieter in Level Flight than in $-6^\circ$ Descending Flight	-3.6	-13.6	-3.9	-5.6	-5.3	-9.2	1.1	-1.1	-3.6	
I	In $-6^\circ$ Descending and Accelerating Flight, Retreating Side Turns are Quieter than Advancing Side Turns	-2.8	-11.5	1.0	-0.4	-6.2	-1.3	-0.6	-8.9	-2.7	
J	In $-3^\circ$ Descending Flight, Retreating Side Turns are Quieter than Advancing Side Turns	-7.9		-1.9	-0.6	-1.9		-1.3	-5.2		
K	In $-6^\circ$ Descending Flight, Retreating Side Turns are Quieter than Advancing Side Turns	-2.7	-3.6	-1.3	-1.2	0.8	-4.1	-4.4	-0.6	-0.6	
L	In $-9^\circ$ Descending Flight, Retreating Side Turns are Quieter than Advancing Side Turns	-1.7	-0.8	-2.0	-3.9	-2.5	-3.3				

correct location. While flying in free space, the confluence of each of these conditions being met perfectly never occurs. As each of these is varied, either the source noise mechanisms on the vehicle are changed, or the resulting acoustic measurement is modified by directivity, distance, and/or atmospheric absorption.

It is outside the scope of this paper to attempt to predict the source noise mechanisms and recalculate the acoustic footprint for imprecise maneuvers. Meanwhile, the microphone arrays were generally large enough and dense enough to capture the shifting directivity pattern if the vehicle was misaligned with the microphone array when the pilot executed the maneuver. However, a minor adjustment to the peak  $L_{A,max}$  value based on the altitude of the vehicle when the pilot initiated the turn maneuver can be computed. If atmospheric absorption is neglected, then the peak  $L_{A,max}$  can be adjusted by  $20 \times \log_{10}(z_{alt}/z_{ref})$  where  $z_{alt}$  is the vehicle altitude at the height of turn initiation in feet and  $z_{ref}$  is the intended ini-

tiation altitude (400 feet for this test design). Applying this modification individually to each of the maneuvers that were compared to generate Table 1, results in Table 2. Overall this altitude adjustment does not make a significant difference in the ‘true’ or ‘false’ results, but has changed some of the ‘neutral’ values.

The information in Table 2 can be further reduced upon inspection. Conditions (A) and (B) can be combined to conclude that level turns are not generally affected by turning direction. Conditions (C) and (D) suggest that level accelerating turns are generally quieter than level decelerating turns. Conditions (E) and (F) suggest that accelerating descents are generally louder than constant speed descents. Conditions (G) and (H) suggest that level turns are quieter than descending turns, while (I) suggests that accelerating descending turns toward the retreating side are generally quieter than similar turns toward the advancing side. Conditions (J) through (L) suggest that constant speed descending turns toward the re-

treating side are quieter than similar turns toward the advancing side, at all descent angles.

This reduced set of guidance has been provided to the Helicopter Association International and has already been implemented in their Fly Neighborly training (Ref. 32). This guidance provides actionable advice to pilots with reasonable fidelity and without substantially increasing pilot workload. While this guidance works well, as evidenced in the previous tables, it may not improve the acoustic footprint for all vehicles. However, it can generally be said that the guidance has not been shown to increase the acoustic footprint, and so performing these maneuvers is the “neighborly” option.

## Conclusions and Future Research

An extensive flight test campaign has been conducted to develop actionable advice for pilots of today’s vehicles to reduce their acoustic footprints. Altogether, 10 vehicles were tested at three different test ranges, with 9 of the vehicles’ data documented here. There were at least 24 turning conditions tested, which was reduced down to 12 pairs of test conditions.

Each turning flight condition was evaluated to determine the peak measured  $L_{A,max}$  value, and the difference between peak values was investigated. That peak value difference was also corrected by the offset from the intended vehicle altitude at turn initiation from the true altitude at initiation. The corrected amplitudes were investigated and grouped into 6 generic guidance principals that can be given to pilots to reduce their acoustic footprint during operations. That vehicle generic guidance is:

- Noise from level flight turns are not affected by turn direction.
- Level accelerating turns are quieter than level decelerating turns.
- Level flight turns are quieter than descending turns.
- Accelerating, descending turns are louder than constant speed descending turns.
- Accelerating, descending turns toward the retreating side are quieter than similar turns toward the advancing side.
- Constant speed, descending turns toward the retreating side are quieter than similar turns toward the advancing side.

While this guidance is useful to today’s pilots operating current fleet vehicles, there is still a substantial amount of work to be done. First, the aerodynamic premise of this guidance is that the pilot has the ability to influence the location and interaction of the blade-vortex interaction, which results in a significant change in the acoustic footprint of the vehicle. However, it is possible the peak  $L_{A,max}$  metric does not accurately capture the impact of the blade-vortex interaction noise, which may be more accurately captured using a metric such

as one using Stephenson’s blade-vortex extraction technique or the blade-vortex interaction sound pressure level (Ref. 26). Furthermore, the peak  $L_{A,max}$  metric does not have a time component associated with it. It is possible that the community is more annoyed by a lower peak  $L_{A,max}$  value that occurs for a longer duration. Therefore, other acoustic metrics must be employed to determine if the guidance provided here and in Ref. 32 remains valid. Finally, this guidance is appropriate for the current, single-main rotor vehicles and does not necessarily apply to the multirotor concepts currently under development for advanced air mobility vehicles.

## References

- <sup>1</sup>Watts, M. E., Greenwood, E., Smith, C., and Stephenson, J., “Noise Abatement Flight Test Data Report,” Technical Memorandum NASA/TM-2019-220264, NASA Langley Research Center, Hampton, VA 23681, USA, March 2019.
- <sup>2</sup>Pascioni, K. A., Greenwood, E., Watts, M. E., Smith, C. D., and Stephenson, J. H., “Medium-Sized Helicopter Noise Abatement Flight Test Data Report,” Technical Memorandum, NASA Langley Research Center, Hampton, VA 23681, USA, 2020.
- <sup>3</sup>Lin II, R.-G., “L.A. County backs federal restriction of low-flying helicopters,” *LA Times*, November 2011.
- <sup>4</sup>Vail, E., “Adopt Local Law- Amending Chapter 75 (Airport) of the Town Code Regulating Nighttime Operation of Aircraft at East Hampton Airport,” East Hampton Town Board Resolution 2015-411, 2015.
- <sup>5</sup>Cox, C. R., “Helicopter Noise Reduction and Its Effects on Operations,” *Journal of the American Helicopter Society*, Vol. 15, (1), 1970, pp. 59–65.
- <sup>6</sup>Gordon, A. C., “Noise and the helicopter pilot (Pilot operation practices for helicopter noise level reduction, with emphasis on flight altitude increase and routing over noise insensitive areas),” *Aeronautical Journal*, Vol. 77, 1973, pp. 220–224.
- <sup>7</sup>Stepniewski, W. Z. and Schmitz, F. H., “Possibilities and problems of achieving community noise acceptance of VTOL,” *The Aeronautical Journal*, Vol. 77, (750), 1973, pp. 311–326.
- <sup>8</sup>Helicopter Association International Fly Neighborly Committee, *Fly Neighborly Guide*, Helicopter Association International, 2007.
- <sup>9</sup>Schmitz, F. H. and Sim, B. W.-C., “Acoustic Phasing, Directionality and Amplification Effects of Helicopter Blade–Vortex Interactions,” *Journal of the American Helicopter Society*, Vol. 46, (4), October 2001, pp. 273–282.
- <sup>10</sup>Schmitz, F. H., “Reduction of Blade-Vortex Interaction (BVI) Noise through X-Force Control,” *Journal of the American Helicopter Society*, Vol. 43, (1), 1998, pp. 14–24.

- <sup>11</sup>Greenwood, E. and Schmitz, F. H., “Effects of Ambient Conditions on Helicopter Rotor Source Noise Modeling,” *Journal of Aircraft*, Vol. 51, (1), January 2014, pp. 90–103.
- <sup>12</sup>Watts, M., Greenwood, E., and Stephenson, J., “Measurement and Characterization of Helicopter Noise at Different Altitudes,” American Helicopter Society 72nd Annual Forum, May 2016.
- <sup>13</sup>Greenwood, E., Sim, B., and Boyd, D., “The Effects of Ambient Conditions on Helicopter Harmonic Noise Radiation,” American Helicopter Society 72nd Annual Forum, May 2016.
- <sup>14</sup>Jacobs, E. W., Prillwitz, R. D., Chen, R. T. N., Hindson, W. S., and Santa Maria, O. L., “The Development and Flight Test Demonstration of Noise Abatement Approach Procedures for the Sikorsky S-76,” AHS Technical Specialists’ Meeting for Rotorcraft Acoustics and Aerodynamics, October 1997.
- <sup>15</sup>Schmitz, F. H., Greenwood, E., Sickenberger, R. D., Gopalan, G., Sim, B. W.-C., Conner, D. A., Morales, E., and Decker, W., “Measurement and Characterization of Helicopter Noise in Steady-State and Maneuvering Flight,” American Helicopter Society 63rd Annual Forum, May 2007.
- <sup>16</sup>Schmitz, F. H., Gopalan, G., and Sim, B. W.-C., “Flight-Path Management/Control Methodology to Reduce Helicopter Blade-Vortex Interaction Noise,” *Journal of Aircraft*, Vol. 39, (2), 2002, pp. 193–205.
- <sup>17</sup>Greenwood, E., Schmitz, F. H., Gopalan, G., and Sim, B., “Helicopter External Noise Radiation in Turning Flight: Theory and Experiment,” Proceedings of the 63<sup>rd</sup> Annual Forum of the American Helicopter Society, Virginia Beach, VA, May 2007.
- <sup>18</sup>Sickenberger, R. D., Gopalan, G., and Schmitz, F. H., “Helicopter Near-Horizon Harmonic Noise Radiation due to Cyclic Pitch Control,” American Helicopter Society 67th Annual Forum, May 2011.
- <sup>19</sup>Greenwood, E., Schmitz, F. H., and Sickenberger, R. D., “A Semiempirical Noise Modeling Method for Helicopter Maneuvering Flight Operations,” *Journal of the American Helicopter Society*, Vol. 60, (2), 2015, pp. 1–13.
- <sup>20</sup>Sickenberger, R. D., *Modeling Helicopter Near-Horizon Harmonic Noise due to Transient Maneuvers*, Ph.D. thesis, University of Maryland, May 2013.
- <sup>21</sup>Spiegel, P., Buchholz, H., and Pott-Pollenske, M., “Highly instrumented BO-105 and EC135-FHS aeroacoustic flight tests including maneuver flights,” Proceedings of the 61<sup>st</sup> Annual Forum of the American Helicopter Society, Grapevine, TX, May 2005.
- <sup>22</sup>Duc, A. L., Spiegel, P., Guntzer, F., Lummer, M., Buchholz, H., and Götz, J., “Simulation of Complete Helicopter Noise in Maneuver Flight using Aeroacoustic Flight Test Database,” American Helicopter 64th Annual Forum, April 2008.
- <sup>23</sup>Guntzer, F., Spiegel, P., and Lummer, M., “Genetic Optimizations of EC-135 Noise Abatement Flight Procedures using an Aeroacoustic Database,” 35th European Rotorcraft Forum, September 2009.
- <sup>24</sup>Watts, M. E., Snider, R., Greenwood, E., and Baden, J., “Maneuver Acoustic Flight Test of the Bell 430 Helicopter,” Proceedings of the 68<sup>th</sup> Annual Forum of the American Helicopter Society, Ft. Worth, TX, May 2012.
- <sup>25</sup>Watts, M. E., Greenwood, E., Smith, C. D., Snider, R., and Conner, D. A., “Maneuver Acoustic Flight Test of the Bell 430 Helicopter Data Report,” Technical Memorandum NASA/TM-2014-218266, NASA Langley Research Center, Hampton, VA 23681, USA, May 2014.
- <sup>26</sup>Stephenson, J. H., *Extraction of Blade Vortex Interactions from Helicopter Transient Maneuvering Noise*, Ph.D. thesis, University of Texas at Austin, 2014.
- <sup>27</sup>Greenwood, E. and Rau, R., “A Maneuvering Flight Noise Model for Helicopter Mission Planning,” *Journal of the American Helicopter Society*, Vol. 65, (2), 2020, pp. 1–10.
- <sup>28</sup>Greenwood, E. and Schmitz, F. H., “A Parameter Identification Method for Helicopter Noise Source Identification and Physics-Based Semiempirical Modeling,” *Journal of the American Helicopter Society*, Vol. 63, (3), 2018, pp. 1–14.
- <sup>29</sup>Gennaretti, M., Bernardini, G., Serafini, J., Anobile, A., and Hartjes, S., “Helicopter noise footprint prediction in unsteady maneuvers,” *International Journal of Aeroacoustics*, Vol. 16, (3), 2017, pp. 165–180.
- <sup>30</sup>Greenwood, E., “Helicopter Flight Procedures for Community Noise Reduction,” Proceedings of the 73<sup>rd</sup> Annual Forum of the American Helicopter Society, Ft. Worth, TX, May 2017.
- <sup>31</sup>Pascioni, K. A., Greenwood, E., Watts, M. E., Smith, C. D., and Stephenson, J. H., “Medium-Sized Helicopter Noise Abatement Flight Test,” Proceedings of the 76<sup>th</sup> Annual Forum of the Vertical Flight Society, Virginia Beach, VA, October 2020.
- <sup>32</sup>Helicopter Association International, *Fly Neighborly Helicopter Noise Abatement Recommendations*, Available at: [https://www.rotor.org/Portals/0/Fly Neighborly/FN Tips Flyer\\_080718\\_with FAA HAI Logo.pdf](https://www.rotor.org/Portals/0/Fly Neighborly/FN Tips Flyer_080718_with FAA HAI Logo.pdf), Accessed on 18-09-2019.